Crystallographic Elucidation of Aluminium Bound Amido Schiff Base Chemosensor: A Selective Turn-on Fluorescent Chemosensor for Al^{3+} ion

Anamika Hoque,[a] Md. Sanaul Islam,[a] Samim Khan,[a] Basudeb Datta,[a] Ennio Zangrando[b]*, Goutam Kumar Kole[c]*, Md. Akhtarul Alam[a]*

[a]Department of Chemistry, Aliah University, Action Area IIA/27, New Town, Kolkata 700160, India.

[b]Department of Chemical and Pharmaceutical Sciences, University of Trieste, Via L. Giorgieri 1, 34127 Trieste, Italy.

[c]Department of Chemistry, SRM Institute of Science and Technology, Kattankulathur, Tamil Nadu 603203, India.

E-mail: ezangrando@units.it (E.Z.), goutamks@srmist.edu.in and alam_iitg@yahoo.com (M.A.A.)

Table of Contents

1. Crystal structure:

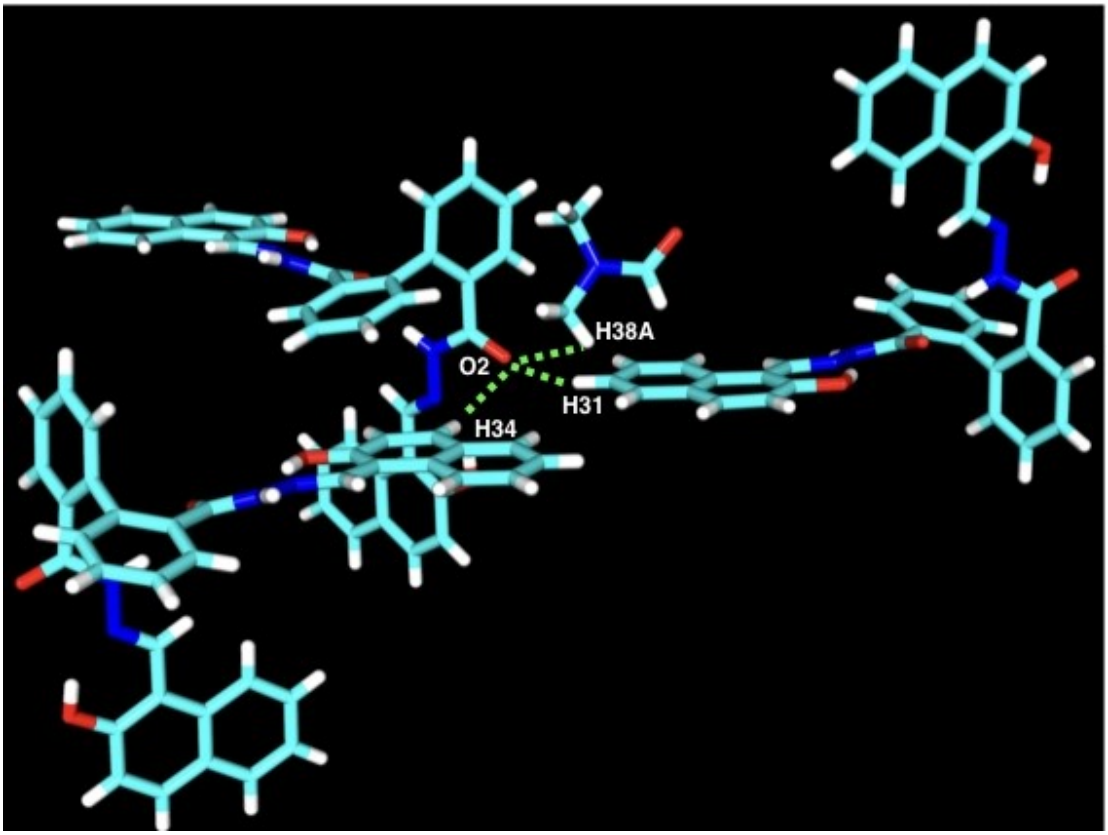

Figure S1. Perspective views of C-H···O hydrogen-bonding interactions in the crystal of sensor **1**.

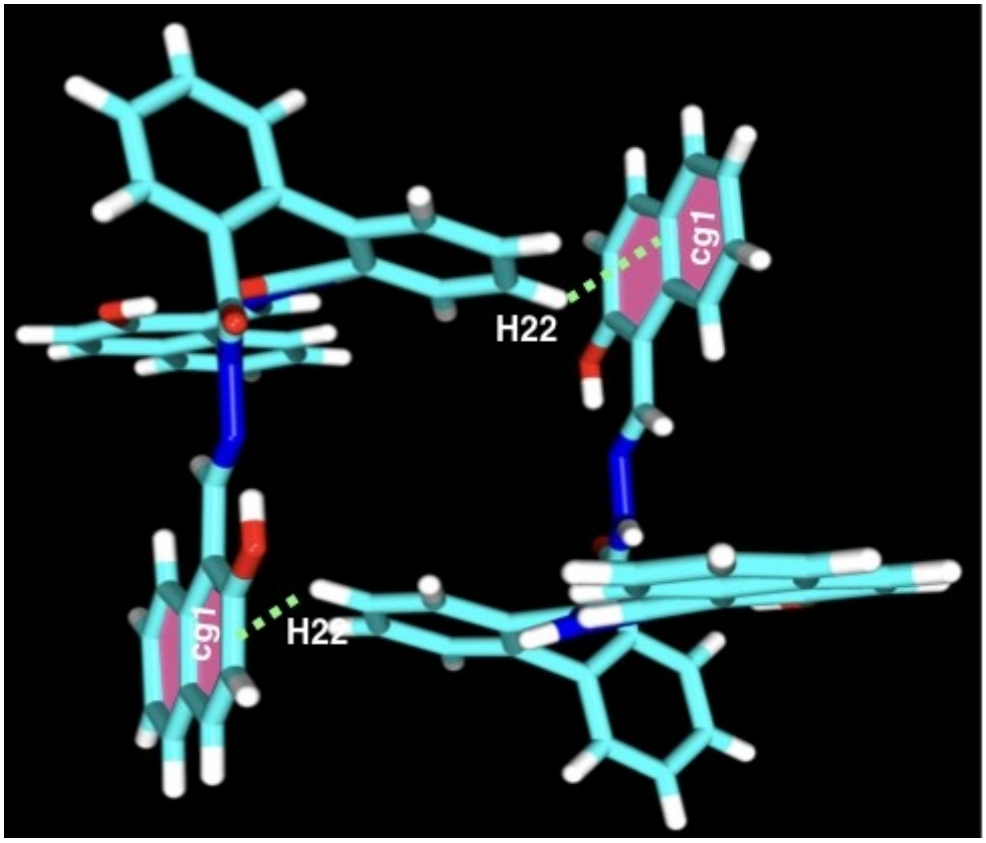

Figure S2. Views of C-H···π interactions between molecules of sensor **1** arranged about an inversion center, solvents are omitted for clarity.

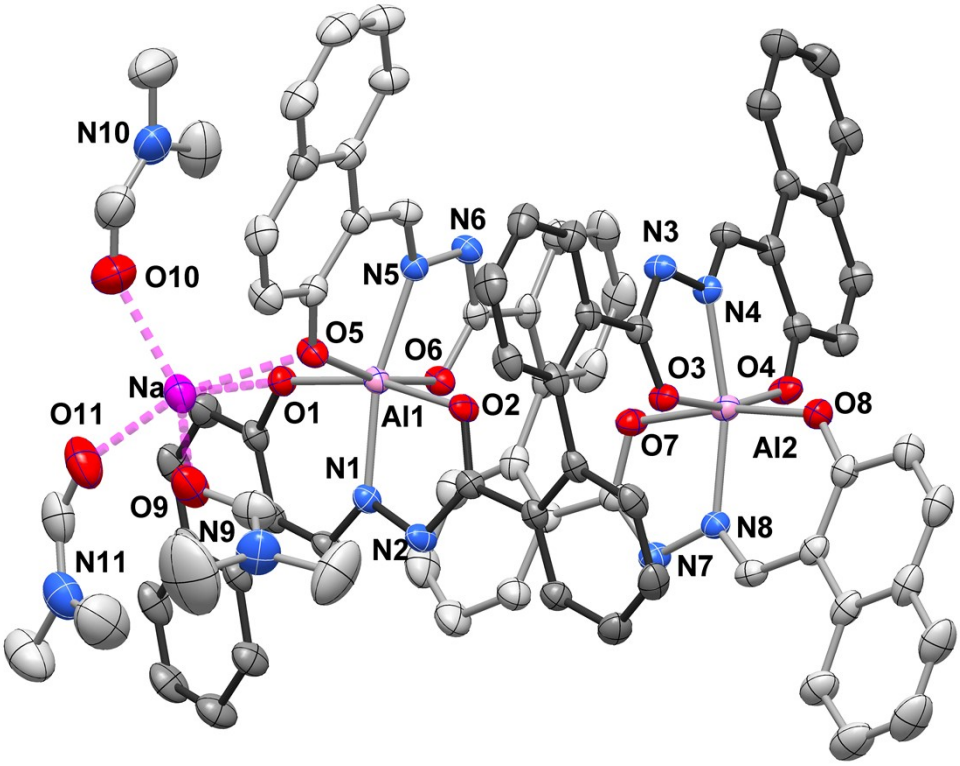

Figure S3. ORTEP representation of complex **1** (probability ellipsoids at 35%) with atom-numbering scheme of coordinating atoms. The two ligands are indicated in different colour. (H atoms, lattice DMF and water molecules not shown for clarity).

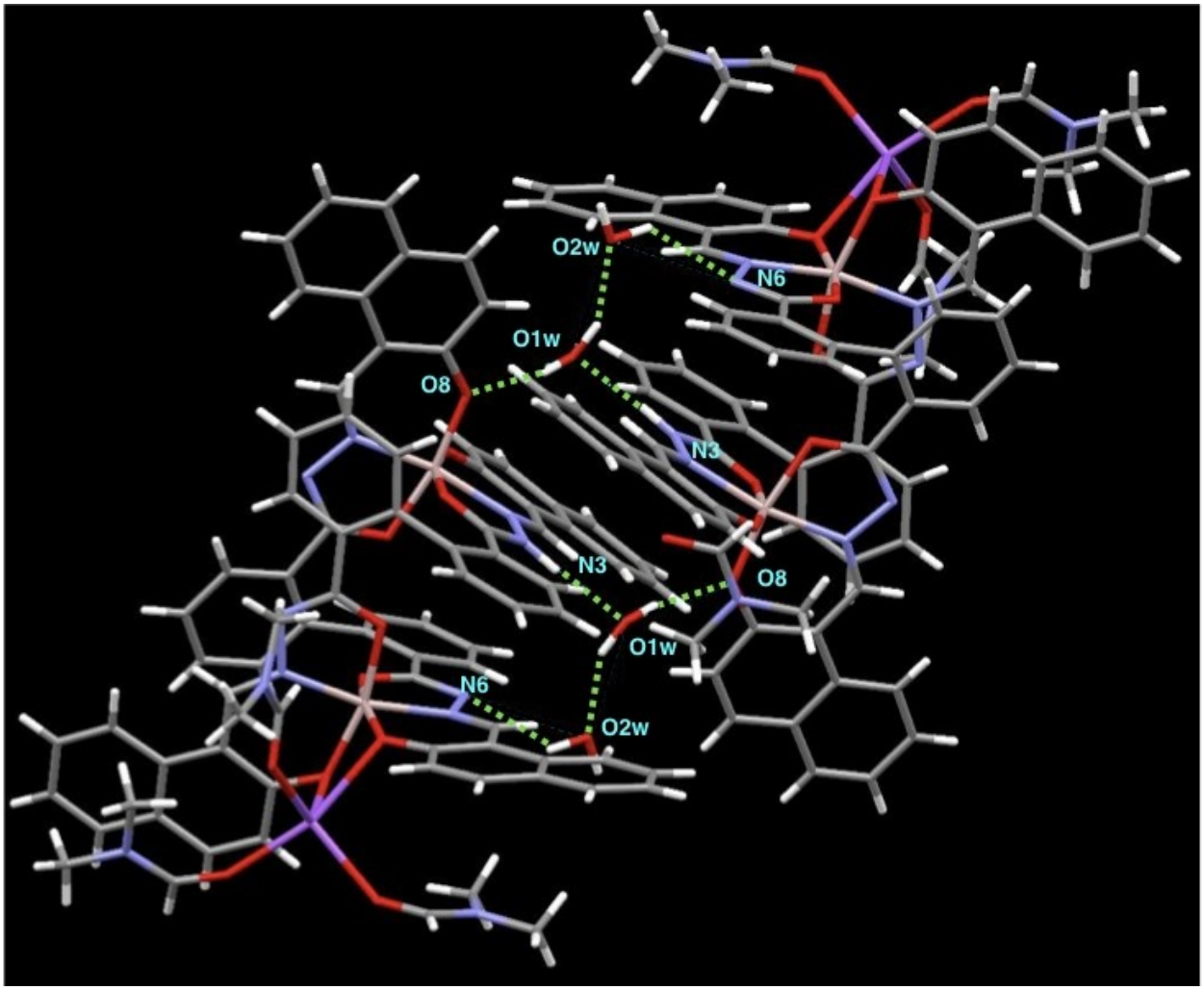

Figure S4. H- bonding network in complex **1** with selected atom-numbering scheme.

2. Powder X-ray diffraction (PXRD):

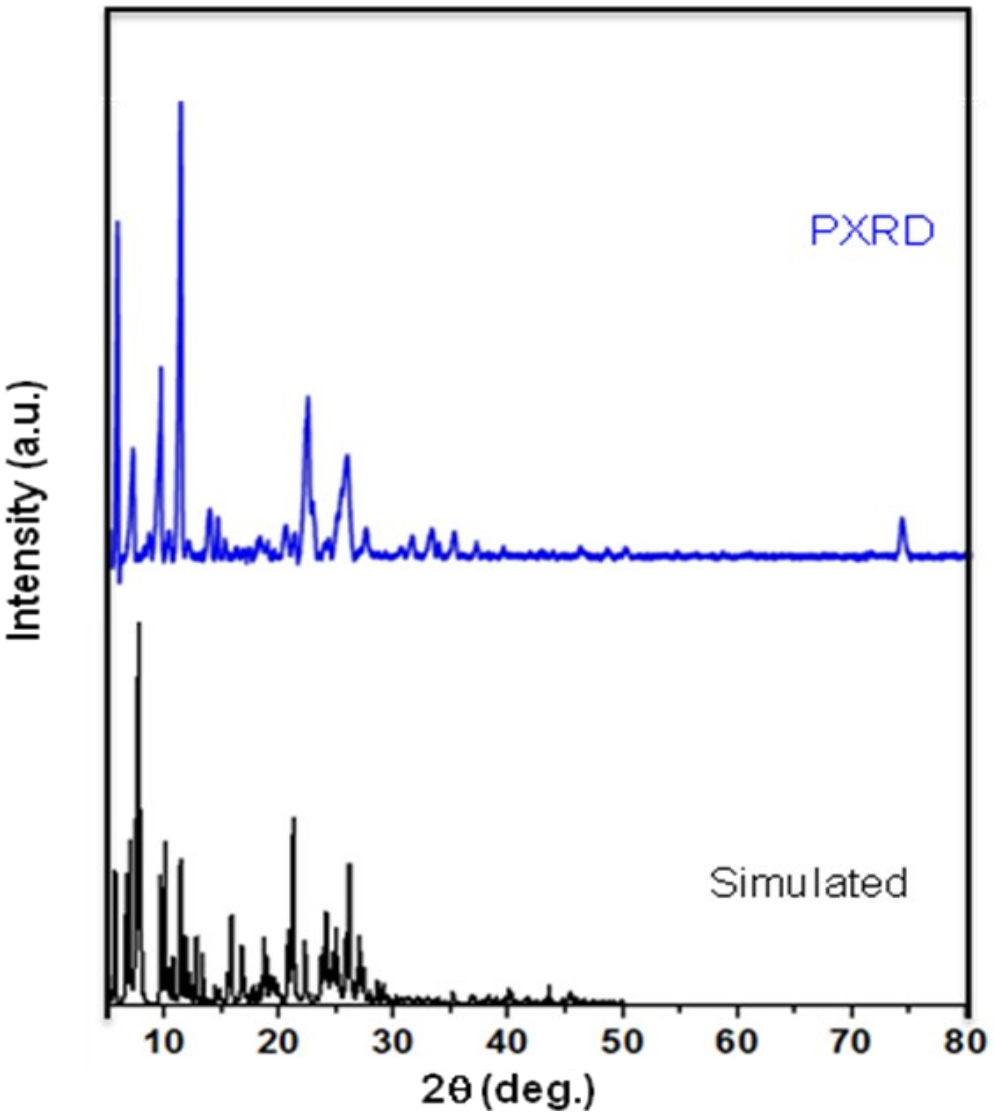

Figure S5. Comparison of PXRD patterns of complex **1** (blue) with the simulated pattern from the single crystal structure of complex **1** (black).

3. UV-vis spectra:

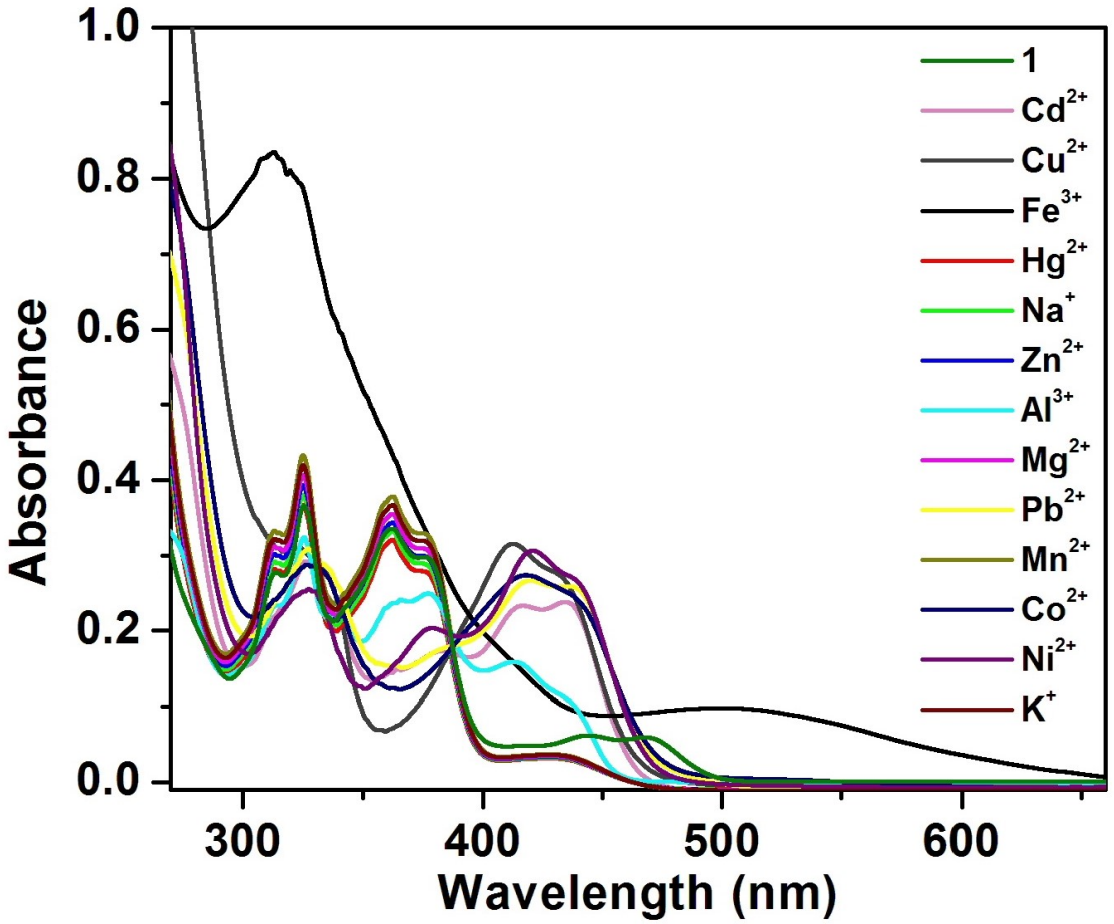

Figure S6. UV-vis spectra of sensor **1** (1×10^{-5} M) in DMF:H_2O solution (7/3, v/v) in presence of different metal ions (2 equivalents).

4 . Fluorescence spectra:

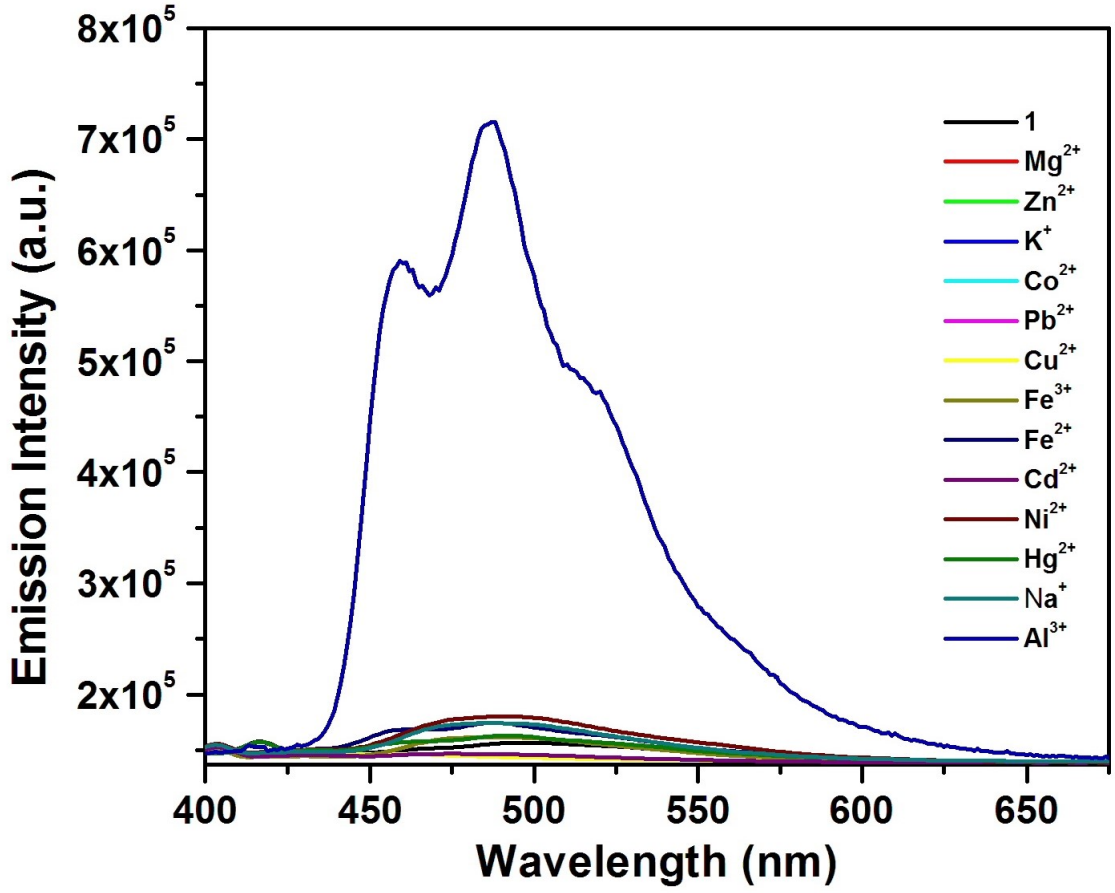

Figure S7. Fluorescence emission spectra of sensor **1** (1×10^{-6} M) in DMF–H_2O solution (7/3, v/v, in presence of different metal ions (2 equivalents) (λ_{ex} = 350 nm).

5. Benesi-Hildebrand Plot:

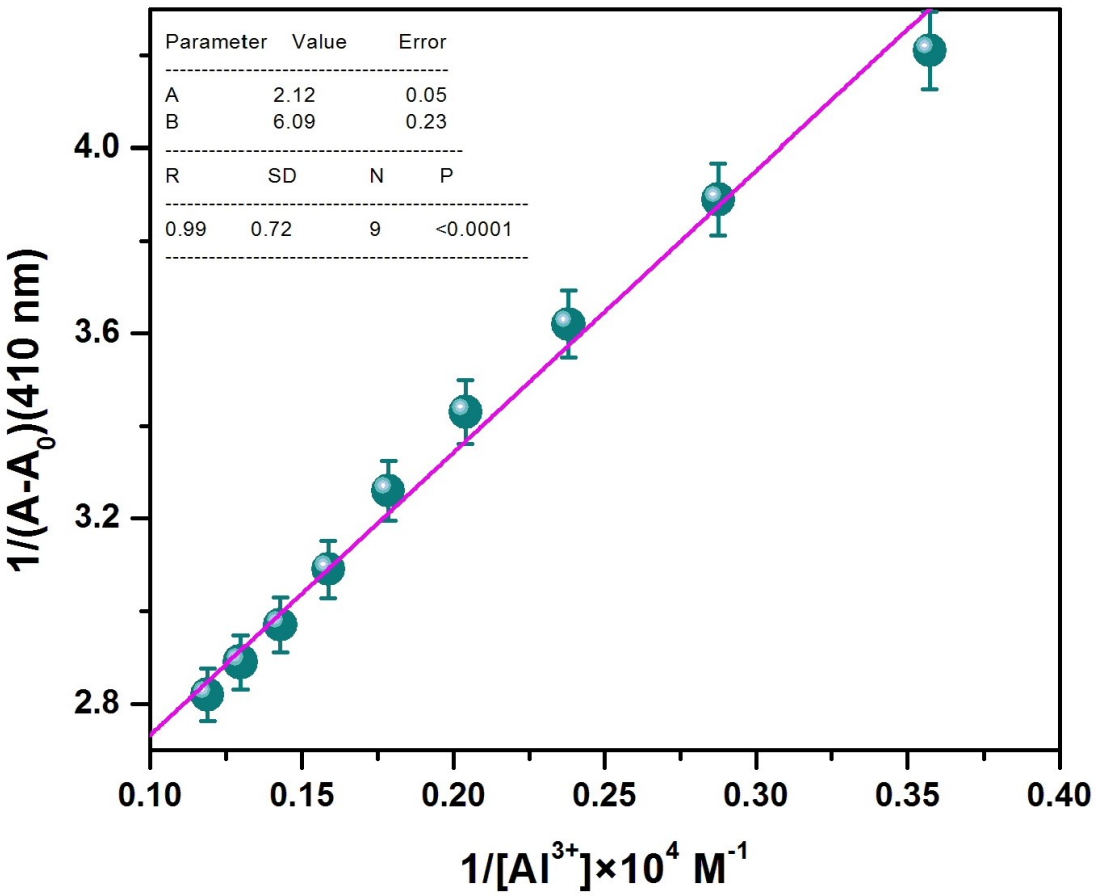

Figure S8. B–H plot for UV-Vis titration of sensor **1** with Al^{3+} ions.

6. Detection limit:

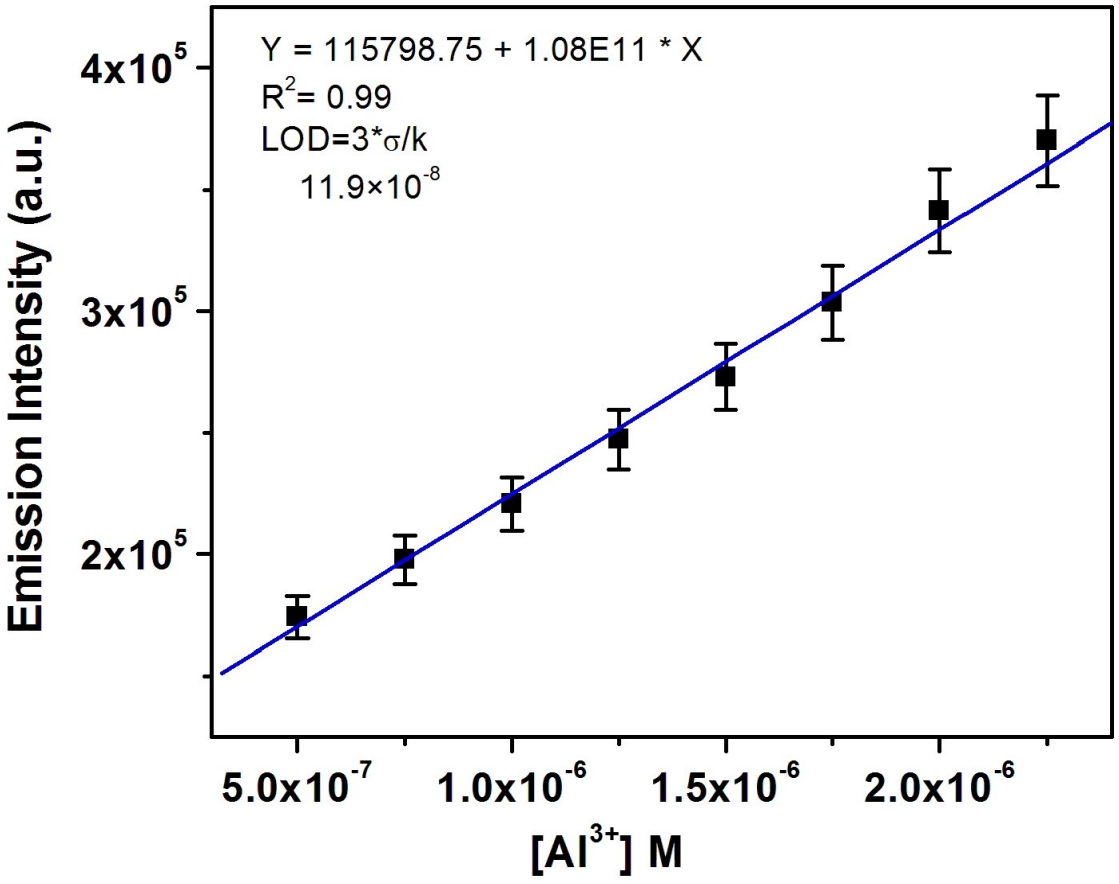

Figure S9. Detection limit of Al^{3+} by sensor **1** based on 3σ/slope.

7. ^{1}H NMR titration spectra:

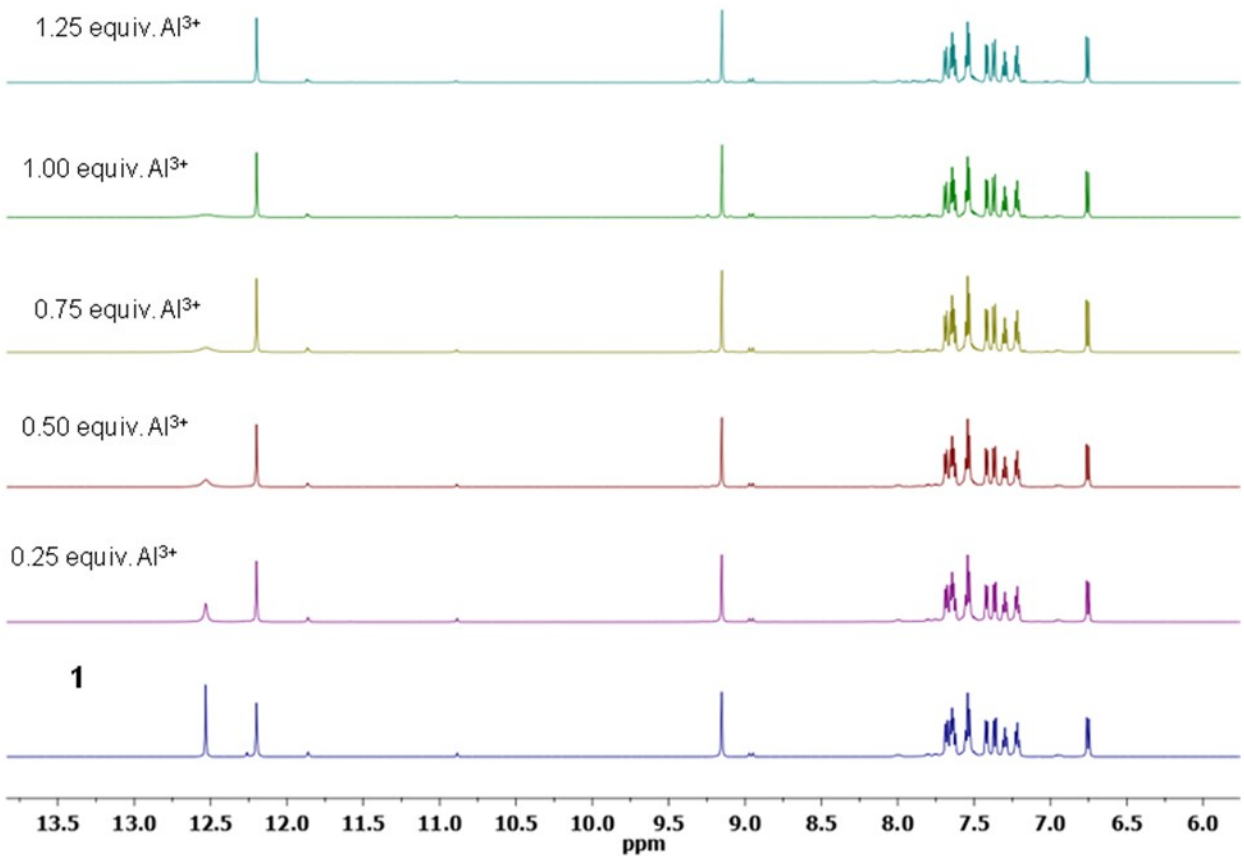

Figure S10. Partial ^{1}H NMR titration spectra of sensor **1** in d_6-DMSO upon addition of different amount of Al^{3+} ions.

8. Job's plot:

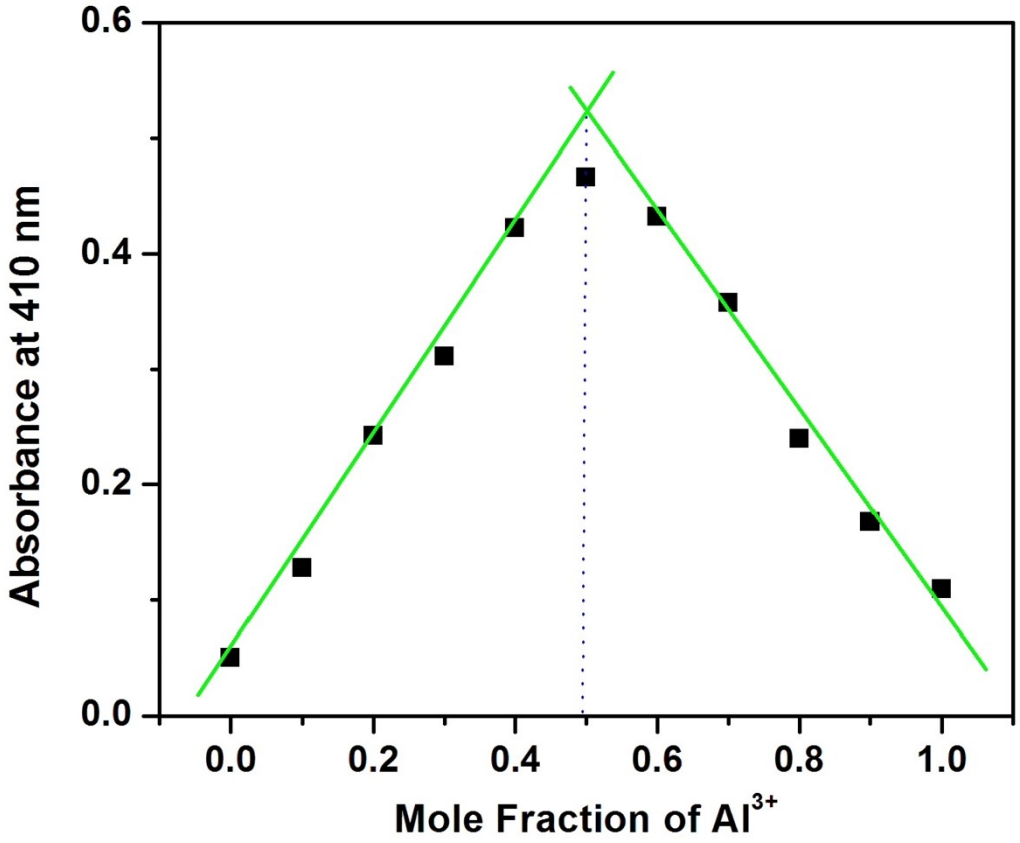

Figure S11. Job's plot for determining the stoichiometry of sensor **1** and Al^{3+} ion in the complex.

9. Mass spectra:

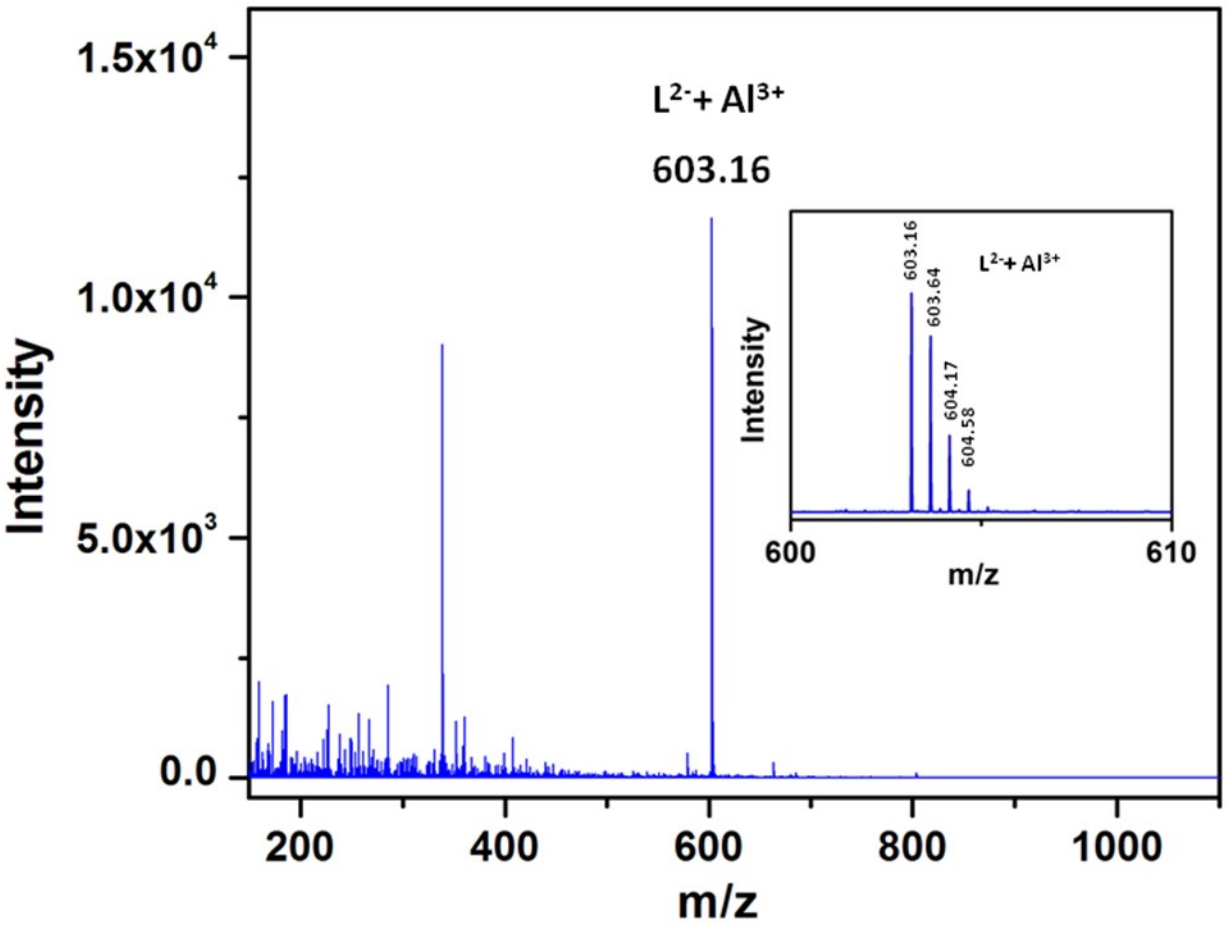

Figure S12. Mass spectrum of complex formed between sensor **1** and Al^{3+} ion.

10. Effect of pH:

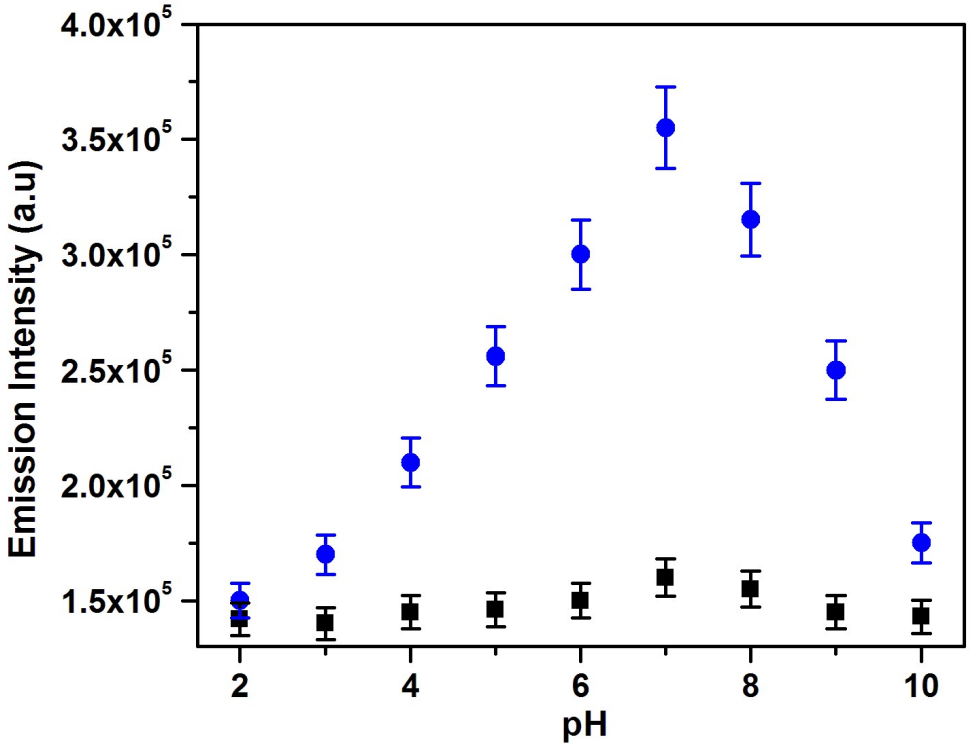

Figure S13. Change in fluorescence intensity sensor **1** (1×10^{-6} M) (■) and its Al^{3+} (●) complex at different pH values.

11. Competition experiment:

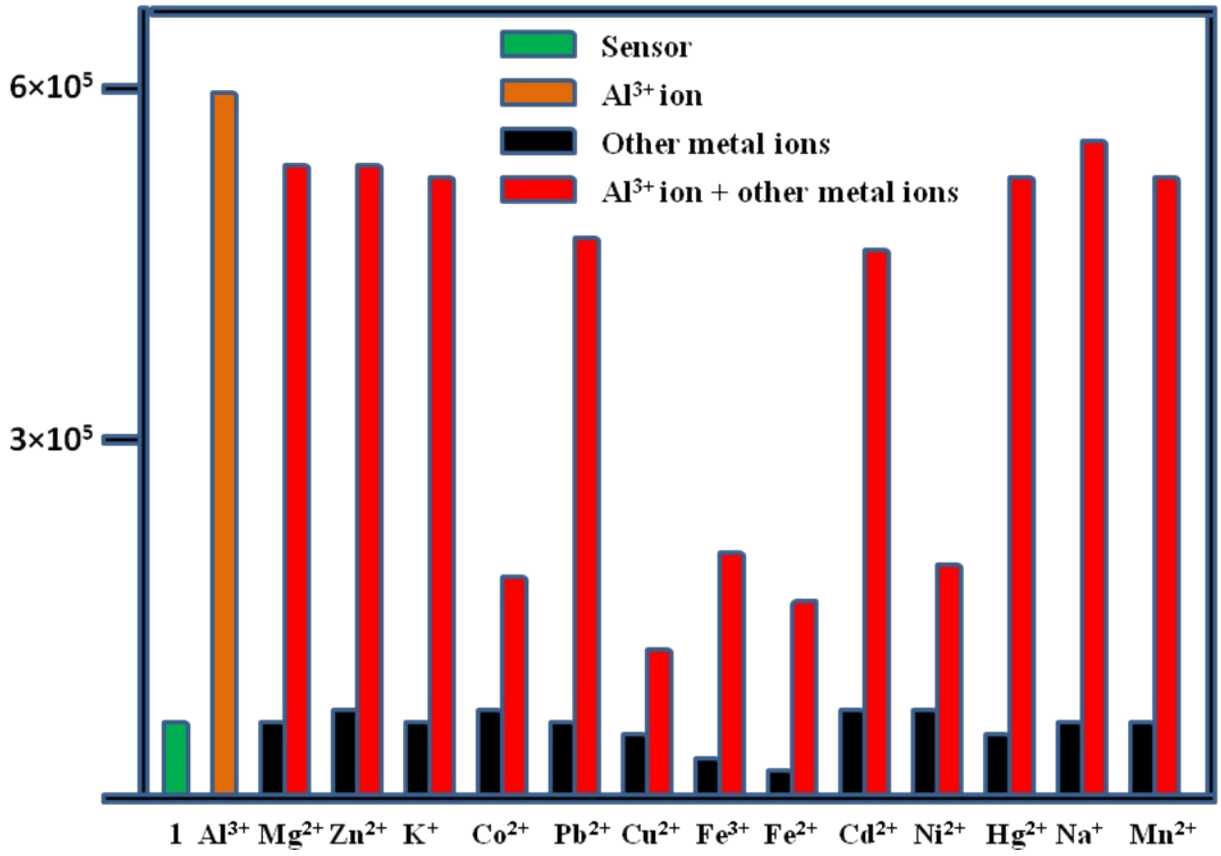

Figure S14. Competition experiments of sensor **1**: plot of fluorescence intensity at 487 nm of sensor **1** with addition of 2.0 equiv. of Al^{3+}, and then 5.0 equiv. of various metal ions, (λ_{ex}: 350 nm).

12. UV-Vis titration with Na_2EDTA:

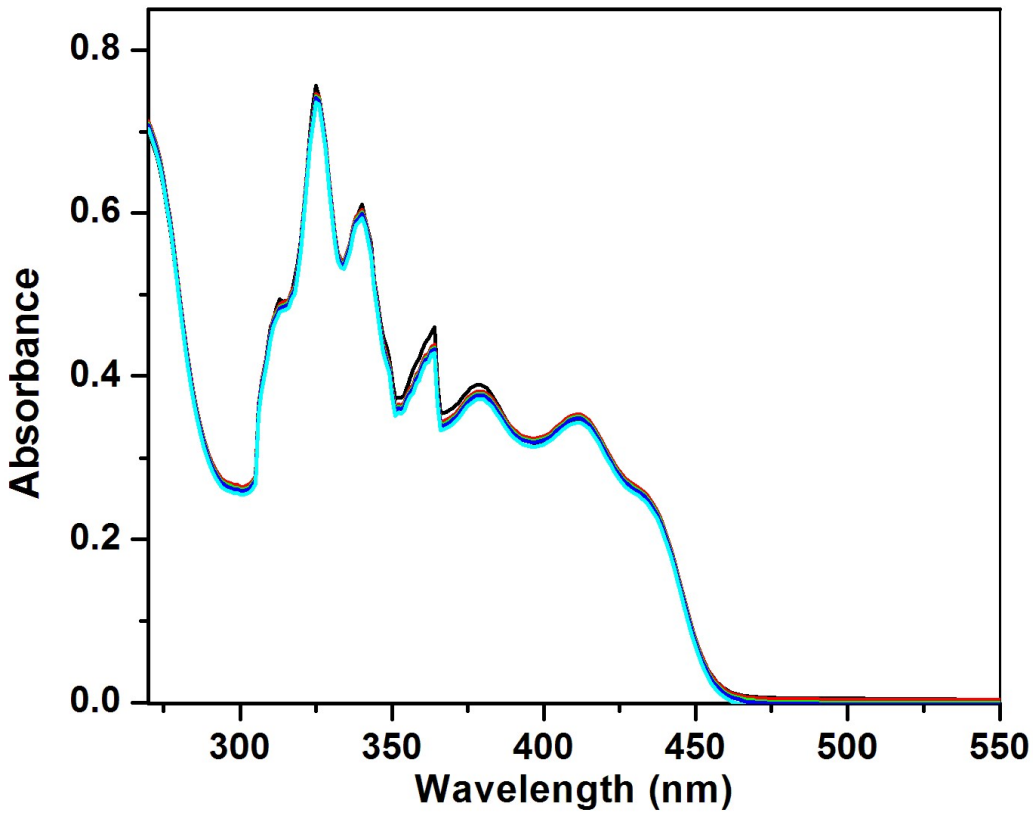

Figure S15. UV-Vis titration of complex **1** with Na_2EDTA (0-5 equivalents) in DMF- H_2O solvent (v/v, 7:3).

13. Fluorescence titration with Na_2EDTA:

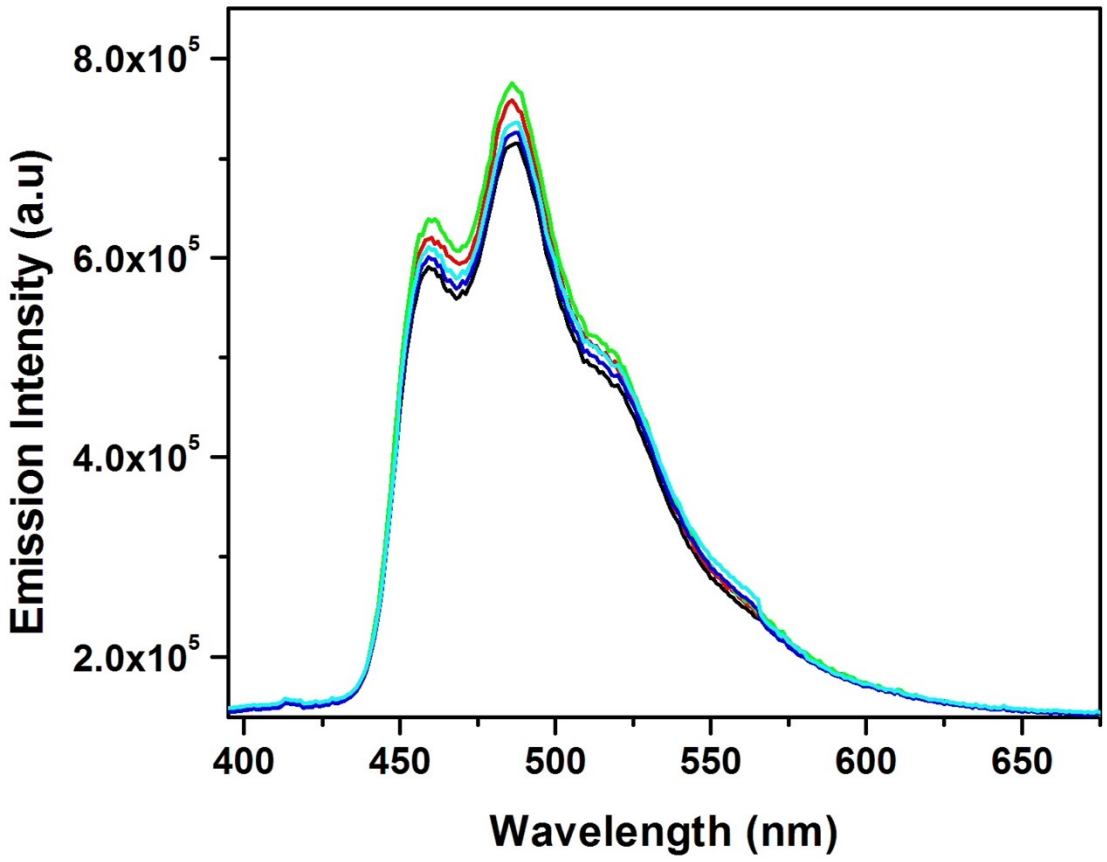

Figure S16. Fluorescence titration of complex **1** in DMF- H_2O solvent (v/v, 7:3) upon addition of (0-5 equivalents) of Na_2EDTA.

14. Table for crystal structure data:

Table S1. Crystal data and structure refinement for Sensor **1** and Complex **1**

	Sensor **1**	Complex **1**
CCDC No.	2260347	2260348
Empirical formula	$C_{39}H_{35}N_5O_6$	$C_{84}H_{77}Al_2N_{12}NaO_{14}$
Formula weight	669.72	1518.97
Temperature/ K	150	273
Crystal system	monoclinic	triclinic
Crystal colour	colourless	light yellow
Space group	*I* 2/a	*P* -1
a/ Å	19.0312(6)	14.5165(4)
b/ Å	15.6836(5)	16.0763(5)
c/ Å	24.3420(6)	18.1614(5)
α/ °	90	81.998(1)
β/ °	110.365(3)	69.664(1)
γ/ °	90	75.218(1)
Volume/ Å^3	6811.4(4)	3836.68(19)
Z	8	2
ρ_{calc}g/cm^3	1.306	1.346
μ/ mm^{-1}	0.090	0.119
F(000)	2816	1628
Index Ranges		
h	$-24 \le h \le 24$	$-17 \le h \le 17$
k	$-20 \le k \le 20$	$-19 \le k \le 19$
l	$-31 \le l \le 31$	$-22 \le l \le 22$
Reflections collected	12675	117151
Independent reflections	7397	14556
Parameters refined	461	998
Goodness-of-fit on F^2	1.050	1.067
Final R1, wR2 indexes [$I>2\sigma(I)$]	0.0569, 0.1355	0.0837, 0.1996
Final R1, wR2 indexes [all data]	0.0801, 0.1553	0.1185, 0.2233
Residuals/ e. Å^{-3}	0.302, -0.239	1.065, -0.998

Table S2. Selected bond distances (Å) and angles (°) for sensor **1** and complex **1**

Bond distances of Sensor **1**			
O(1)-C(1)	1.349(3)	O(3)-C(25)	1.228(2)
O(2)-C(12)	1.226(2)	O(4)-C(36)	1.358(3)
N(1)-C(11)	1.278(3)	N(3)-C(25)	1.367(3)
N(2)-C(12)	1.355(3)	N(4)-C(26)	1.290(3)
Bond distances of Complex **1**			
Al(1)-O(1)	1.882(3)	Al(2)-O(3)	1.957(3)
Al(1)-O(2)	1.904(3)	Al(2)-O(4)	1.833(3)
Al(1)-O(5)	1.855(3)	Al(2)-O(7)	1.877(3)
Al(1)-O(6)	1.880(3)	Al(2)-O(8)	1.845(3)
Al(1)-N(1)	1.986(3)	Al(2)-N(4)	1.993(3)
Al(1)-N(5)	1.991(3)	Al(2)-N(8)	1.956(3)
O(1)-Na	2.518(3)	O(10)-Na	2.288(5)
O(5)-Na	2.407(3)	O(11)-Na	2.248(4)
O(9)-Na	2.352(5)	Al(1)-Na	3.391(2)
Bond angles of Complex **1**			
O(5)-Al(1)-O(6)	165.76(13)	O(4)-Al(2)-O(8)	89.75(13)
O(5)-Al(1)-O(1)	86.88(12)	O(4)-Al(2)-O(7)	92.29(13)
O(6)-Al(1)-O(1)	91.08(12)	O(8)-Al(2)-O(7)	169.62(13)
O(5)-Al(1)-O(2)	92.31(12)	O(4)-Al(2)-N(8)	103.89(13)
O(6)-Al(1)-O(2)	93.32(12)	O(8)-Al(2)-N(8)	89.71(13)
O(1)-Al(1)-O(2)	164.68(12)	O(7)-Al(2)-N(8)	79.92(12)
O(5)-Al(1)-N(1)	100.73(13)	O(4)-Al(2)-O(3)	165.64(12)
O(6)-Al(1)-N(1)	93.19(12)	O(8)-Al(2)-O(3)	89.29(12)
O(1)-Al(1)-N(1)	86.43(12)	O(7)-Al(2)-O(3)	91.23(12)
O(2)-Al(1)-N(1)	78.68(12)	N(8)-Al(2)-O(3)	90.43(12)
O(5)-Al(1)-N(5)	87.85(12)	O(4)-Al(2)-N(4)	87.85(12)
O(6)-Al(1)-N(5)	79.08(12)	O(8)-Al(2)-N(4)	98.79(13)
O(1)-Al(1)-N(5)	105.16(13)	O(7)-Al(2)-N(4)	91.46(12)
O(2)-Al(1)-N(5)	90.08(12)	N(8)-Al(2)-N(4)	165.59(14)
N(1)-Al(1)-N(5)	166.04(14)	O(3)-Al(2)-N(4)	78.14(11)
O(11)-Na-O(10)	98.30(19)	O(9)-Na-O(5)	85.44(14)
O(11)-Na-O(9)	94.07(18)	O(11)-Na-O(1)	100.56(14)
O(10)-Na-O(9)	122.4(2)	O(10)-Na-O(1)	109.03(15)
O(11)-Na-O(5)	158.60(15)	O(9)-Na-O(1)	123.45(16)
O(10)-Na-O(5)	99.99(15)	O(5)-Na-O(1)	62.85(9)

Table S3. Al-O and amide C=O bond lengths (Å) in complex **1** showing the difference between the C25=O3 amide with respect to other amides.

Aluminium atom	-C=O…Al^{3+}	-C=O	Carbonyl-amide -C-NH
Al1	1.904(3)	1.294(4)	1.312(5)
	1.880(3)	1.287(4)	1.314(5)
Al2	1.957(3)	1.251(4)	1.341(4)
	1.877(3)	1.295(4)	1.320(5)

Table S4. Hydrogen bond parameters (Å/°) of sensor **1** and complex **1**.

D-H…A	D-H	H…A	D…A	D-H…A	Symmetry code of A
			Sensor **1**		
O1-H1…N1	0.84	1.82	2.554(2)	146	-
N2-H2N…O3	0.88	1.98	2.833(2)	164	-
N3-H3N…O5	0.88	2.04	2.855(3)	154	-
O4-H4…N4	0.84	1.83	2.568(2)	145	-
O5-H5A…O6	0.87(2)	1.958(19)	2.820(3)	169(4)	-
O5-H5B…O6	0.88(2)	2.013(18)	2.868(2)	163(3)	1/2-x,3/2-y,1/2-z
			Complex **1**		
N3-H3N…O1w	0.89	1.96	2.848(4)	174	-
O1w-H11w…O8	0.85	2.07	2.908(4)	168	1-x,1-y,2-z
O1w-H12w…O2w	0.87	2.08	2.882(6)	151	-
O2w-H21w…N6	0.91	2.26	2.937(6)	130	-
O2w-H22w…O10	0.90	2.716	3.376(6)	131	1-x,1-y,1-z

Table S5. Weak interactions in complex **1**

D-H…A	D-H	H…A	D…A	D-H…A	Symmetry code of A
C23-H23…O1w	0.93	2.59	3.472(6)	158	-
C26-H26…O1w	0.93	2.57	3.347(6)	141	-
C66-H66…O13	0.93	2.52	3.111(13)	122	x,-1+y,z
C88-H88b…O12	0.96	2.24	3.171(14)	164	2-x,1-y,1-z
C91-H91c…O1w	0.96	2.57	3.387(14)	143	1+x,y,z

15. Comparative table:

Table S6: Comparative table of probes previously reported on the basis of their medium, binding constant, limit of detection and application.

	Analyte	Medium	Method	Binding constant $K_{b,}$ (M^{-1})	Detection limit (M)	Applications	Ref.
1	Al^{3+}, F^-	DMSO/ H_2O	Fluorometric	Al^{3+}:8.50 $\times 10^5$	Al^{3+}: 1.05 $\times 10^{-8}$	Logic gate, Live cell imaging	1
2	Al^{3+} $H_3PO_4^-$	CH_3OH	Fluorometric	Al^{3+}: 3.6 $\times 10^4$	Al^{3+}: 8.30 $\times 10^{-7}$ $H_3PO_4^-$: 1.7$\times 10^{-6}$	Paper strips	2
3	Al^{3+}	CH_3OH/H_2O	Fluorometric	5.42 $\times 10^5$	3.55 $\times 10^{-7}$	Paper strips Logic gate	3
4	Al^{3+}	DMSO/H_2O	Fluorometric	4.09 $\times 10^4$	1.20$\times 10^{-7}$	Live cell imaging	4
5	Al^{3+}	DMSO/H_2O	Fluorometric		1.90$\times 10^{-6}$	-	5
6	Al^{3+}	CH_3OH/H_2O	Fluorometric	2.85$\times 10^5$	1.1$\times 10^{-7}$	-	6
7	Al^{3+}	DMF/H_2O	Fluorometric	2.75$\times 10^3$	4.9$\times 10^{-7}$	Paper strips	7
8	Al^{3+}	CH_3OH	Fluorometric	1.6$\times 10^4$	2.7$\times 10^{-7}$	Paper strips	8
9	Al^{3+}	DMSO	Fluorometric	1.4$\times 10^4$	2.0$\times 10^{-7}$	Paper strips	9
10	Al^{3+}	DMF/H_2O	Fluorometric	3.48$\times 10^3$	11.9 $\times 10^{-8}$	Paper strips	This work

16. References:

1 D. Sarkar, P. Ghosh, S. Gharami, T.K. Mondal and N. Murmu, A novel coumarin based molecular switch for the sequential detection of Al^{3+} and F^{-}: Application in lung cancer live cell imaging and construction of logic gate, *Sens Actuators B Chem*., 2017, **242**, 338–346.

2 D. Choe and C. Kim, An acylhydrazone-based fluorescent sensor for sequential recognition of Al^{3+} and H_2PO_4, *Materials,* 2021, **14**, 6392.

3 G. Bartwal, K. Aggarwal and J.M. Khurana, An ampyrone based azo dye as pH-responsive and chemo-reversible colorimetric fluorescent probe for Al^{3+} in semi-aqueous medium: implication towards logic gate analysis, *New J. Chem.,* 2018, **42**, 2224–2231.

4 A. Saravanan, S. Shyamsivappan, N. Kalagatur, T. Suresh, N. Maroli, N. Bhuvanesh, P. Kolandaivel and P. Mohan, Application of real sample analysis and biosensing: synthesis of new naphthyl derived chemosensor for detection of Al^{3+} ions, *Spectrochim. Acta A,* 2020, **241**, 118684.

5 R. Shanmugapriya, P. Kumar, K. Poongodi, C. Nandhini and K.P. Elango, 3-Hydroxy- 2-naphthoic hydrazide as a probe for fluorescent detection of cyanide and aluminium ions in organic and aquo-organic media and its application in food and pharmaceutical samples, *Spectrochim. Acta A,* 2021, **249**, 119315.

6 V. Kumar, S. Kundu, B. Sk and A. Patra, A naked-eye colorimetric sensor for methanol and 'turn-on' fluorescence detection of Al^{3+}, *New J. Chem.,* 2019, **43**, 18582–18589.

7 A. Mondal, E. Ahmmed, S. Chakraborty, A. Sarkar, S. Lohar and P. Chattopadhyay, Aggregation induced emission enhancement (AIEE) of naphthalene appended organic moiety: An Al^{3+} ion selective turn on fluorescent probe, *Chemistry Select*, 2020, **5**, 147 –155.

8 G. Kumar, K. Paul and V. Luxami, Aggregation induced emission -excited state intramolecular proton transfer based "off-on" fluorescent sensor for Al^{3+} ions in liquid and solid state, *Sens. Actuators B. Chem.,* 2018, **263**, 585 –593.

9 X. Mei Jiang, W.H. Mi, W. Zhu, H. Yao, Y.M. Zhang, T.B. Wei and Q. Lin, A biacylhydrazone-based chemosensor for fluorescence 'turn-on' detection of Al^{3+} with high selectivity and sensitivity, *Supramolecular Chemistry*, 2019, **31**, 80–88.